European Journal of Pharmaceutical Sciences 41 (2010) 244–253

Contents lists available at ScienceDirect

European Journal of Pharmaceutical Sciences

journal homepage: www.elsevier.com/locate/ejps

Preparation of nanoparticles by solvent displacement for drug delivery: A shift in the "ouzo region" upon drug loading

Moritz Beck-Broichsitter[1], Erik Rytting[1], Tobias Lebhardt, Xiaoying Wang, Thomas Kissel*

Department of Pharmaceutics and Biopharmacy, Philipps-Universität Marburg, Ketzerbach 63, D-35037 Marburg, Germany

ARTICLE INFO

Article history:
Received 5 October 2009
Received in revised form 12 June 2010
Accepted 14 June 2010
Available online 22 June 2010

Keywords:
Nanoparticles
Solvent displacement
"ouzo effect"
Biodegradable polyesters
Salbutamol
Pulmonary drug delivery

ABSTRACT

As biodegradable nanoparticles meet with increasing interest for drug delivery applications, a series of investigations were carried out to understand the mechanism of the formation of drug-loaded nanoparticles using the solvent displacement method. Although previous explanations referred to Marangoni convection as the driving force for nanoprecipitation, recent publications describing the so-called "ouzo effect" sparked these current studies using a novel negatively charged polymer, poly(vinyl sulfonate-*co*-vinyl alcohol)-*graft*-poly(D,L-lactide-*co*-glycolide) (P(VS-VA)-g-PLGA), and a positively charged model drug, salbutamol. Interfacial tension did not influence the nanoparticle formation as would be expected if governed by Marangoni convection, but ternary phase diagrams outlined the so-called "ouzo regions" defining the polymer and solvent concentrations leading to stable nanoparticle suspensions for both this novel polymer and unmodified poly(D,L-lactide-*co*-glycolide) (PLGA). Physicochemical properties, morphology and drug loading of the nanoparticles were analyzed, and stable P(VS-VA)-g-PLGA nanoparticles with and without salbutamol ranged in size from 59–191 nm. The "ouzo region" phase diagram boundaries shifted considerably upon drug loading, which can be explained by the increased solubility of the polymer–drug complex. This behavior necessitated a substantial adjustment of polymer concentrations required to produce drug-loaded nanoparticles with characteristics comparable to blank nanoparticles. In conclusion, the use of "ouzo diagrams" is a beneficial tool to manufacture nanoparticles with specified physicochemical properties by the solvent displacement method.

1. Introduction

In recent years colloidal carriers have become increasingly attractive options for drug delivery. Numerous investigations have shown that nanoparticles composed of biodegradable polymers possess several advantages, such as improved stability of therapeutic agents against degradation, controlled drug release, cell specific targeted drug delivery or modified biological distribution of drugs, both at the cellular and organ level and fulfil the stringent requirements placed on these delivery systems, such as biocompatibility and degradability within an acceptable period of time (Soppimath et al., 2001; Panyam and Labhasetwar, 2003).

Among the large number of biodegradable polymers available for the preparation of polymeric nanoparticles, those most commonly used belong to the family of polyesters. These polymers are known to exhibit excellent biocompatibility and adequate biodegradation under physiological conditions (Anderson and Shive, 1997). However, linear polyesters such as poly(lactide-*co*-glycolide) (PLGA) have many limitations as nanoparticulate drug delivery systems. Firstly, PLGA nanoparticles degrade over a period of weeks to months, but typically deliver drugs for a much shorter period of time. Such a pattern would lead to an unwanted accumulation of polymer in the body when repeated administrations are needed. One way to overcome this problem is to synthesize polymers with faster degradation rates. Fast degrading polymers, composed of short PLGA chains grafted onto charge-modified poly(vinyl alcohol) backbones, have been designed for drug delivery (Dailey et al., 2005; Rytting et al., 2008).

Secondly, for an effective nanoparticulate delivery system, sufficient drug loading must be ensured. Nanoparticles prepared from hydrophobic polymers, like PLGA, often incur the drawback of poor incorporation of low molecular weight hydrophilic drugs due to the low affinity of the drug compounds to the polymers (Barichello et al., 1999). Recently a new class of negatively charged branched polyesters suitable for nanoparticle production was synthesized, namely poly(vinyl sulfonate-*co*-vinyl alcohol)-*graft*-poly(D,L-lactide-*co*-glycolide), abbreviated as P(VS-VA)-g-PLGA (Wang et al., 2008). The introduction of negatively

* Corresponding author. Tel.: +49 6421 28 25881; fax: +49 6421 28 27016.
E-mail addresses: kissel@staff.uni-marburg.de, kissel@staff.uni-marburg.de (T. Kissel).
[1] These authors contributed equally to this work.

0928-0987/$ – see front matter © 2010 Elsevier B.V. All rights reserved.
doi:10.1016/j.ejps.2010.06.007

charged functional groups within the polymer structure promotes electrostatic interactions with oppositely charged drugs, thereby improving the design of nanoparticulate carriers as drug delivery systems (Jung et al., 2000; Beck-Broichsitter et al., 2010; Rytting et al., 2010).

Several manufacturing techniques, including salting-out, emulsion evaporation, emulsification diffusion, and solvent displacement are used to produce biodegradable nanoparticles from preformed, well-defined polymers (Vauthier and Bouchemal, 2009). The solvent displacement method is a convenient, reproducible, fast, and economic one-step manufacturing process for the preparation of monodisperse, polymeric nanoparticles in a size range of approximately 50–300 nm (Fessi et al., 1989). This technique requires the use of amphiphilic organic solvents that are completely miscible with water, for example acetone. Progressive addition of polymer dissolved in acetone to an aqueous phase under stirring leads to the formation of colloidal particles. The molecular mechanism of instantaneous particle formation involves complex interfacial hydrodynamic phenomena and has been explained by interfacial turbulences between two liquid phases which are governed by the Marangoni effect (Sternling and Scriven, 1959; Quintanar-Guerrero et al., 1998; Galindo-Rodriguez et al., 2004).

However, recent publications promote the "ouzo effect" as the driving the force for nanoparticle formation by solvent displacement (Vitale and Katz, 2003; Ganachaud and Katz, 2005). The "ouzo effect" occurs when a hydrophobic solute is rapidly brought into the metastable region ("ouzo region") between the binodal (miscibility-limit curve) and spinodal (stability-limit curve) boundaries in a ternary phase diagram composed of hydrophobic solute, solvent, and non-solvent. Local supersaturation of hydrophobic solute molecules leads to spontaneous nucleation in the form of small particles that grow with time due to Ostwald ripening (nucleation and growth process) (Sitnikova et al., 2005). Based on these assumptions, polymers can act as hydrophobic solute molecules and the "ouzo effect" can lead to the formation of polymeric nanoparticles (Ganachaud and Katz, 2005).

While there is some overlap in the physical parameters describing Marangoni convection and the "ouzo effect", such as concentration gradients, diffusivity, temperature, and interfacial tension, Sternling and Scriven (1959) refer to the Marangoni effect as "surface tension-driven flow". Specifically, variations in concentration and interfacial tension along an interface cause disturbances in mechanical equilibrium where lower free energy can be achieved by the expansion of regions of low interfacial tension at the expense of adjacent regions of higher tension. In a review of the "ouzo effect", on the other hand, Ganachaud and Katz (2005) point out that spontaneous emulsification has been observed both with and without surfactant in regions far from the critical point, thereby de-emphasizing the importance of interfacial tension to the process.

Despite its relevance for pharmaceutical nanotechnology, the impact of the "ouzo effect" for the preparation of polymeric nanoparticles has been so far rather underestimated. Therefore, studies were undertaken to understand the physicochemical principles associated with nanoparticle production by the solvent displacement method, like solvent type, mixing speed of polymer solution with non-solvent phase, polymer molecular weight, concentration and viscosity of polymer solutions, and interfacial tension of the non-solvent phase. These data were analyzed to discriminate between principles of Marangoni convection and the "ouzo effect" hypothesized to govern nanoparticle formation by this modified solvent displacement method. Depicting a map of compositions, "ouzo diagrams" for a linear polyester (PLGA) and a newly synthesized branched polyester (P(VS-VA)-g-PLGA) are presented. The particle size, particle size distribution, ζ-potential, and particle morphology of the prepared nanoparticles were investigated using photon correlation spectroscopy, laser Doppler anemometry, and atomic force microscopy. Finally, the influence of drug loading on the observed shift in the "ouzo region" for P(VS-VA)-g-PLGA was investigated and nanoparticle drug loadings were assayed by high performance liquid chromatography.

2. Materials and methods

2.1. Materials

Linear polyesters, poly(D,L-lactide-*co*-glycolide) (PLGA, Resomers® RG502H, RG503H, and RG504H), were acquired from Boehringer Ingelheim (Ingelheim, Germany). Branched polyesters, namely poly(vinyl sulfonate-*co*-vinyl alcohol)-*graft*-poly(D,L-lactide-*co*-glycolide), were synthesized and characterized as described previously (Wang et al., 2008). These branched polyesters are comprised of short PLGA chains grafted onto a poly(vinyl sulfonate-*co*-vinyl alcohol) (P(VS-VA)) backbone. The following nomenclature is used to characterize the polymers: P(VS-VA)-g-PLGA-*X*-*Y*. The first number (*X*) designates the ratio of vinyl sulfonate relative to vinyl acetate employed in the backbone synthesis. The second number (*Y*) describes the PLGA grafting ratio. P(VS-VA)-g-PLGA-4-10 was used in this study. The β_2-agonist salbutamol (free base) was a gift from Boehringer Ingelheim (Ingelheim, Germany), and the amphiphilic non-ionic triblock copolymer Pluronic® F68 was purchased from BASF (Ludwigshafen, Germany). All other chemicals and solvents used in this study were of the highest analytical grade commercially available.

2.2. Methods

2.2.1. Physicochemical characterization of polymer solutions

2.2.1.1. Density measurements. All density measurements were performed using an oscillating density meter (DMA 46, Anton Paar, Graz, Austria) at 25 °C. This instrument was calibrated with respect to the densities of water and acetone (calculated at 25 °C using ambient pressure and humidity). Polymer solutions were allowed to equilibrate for 12 h at 25 °C before measurements. The density of each solution was calculated from the average of three repeated measurements.

2.2.1.2. Viscosity measurements. The kinematic viscosities of acetone and polymer solutions employing acetone as solvent were measured at 25 °C using a temperature controlled capillary viscosimeter of the Ubbelohde type (Type No. 53100, Capillary No. 0, Schott, Mainz, Germany). The equipment was calibrated with respect to the viscosities of water and acetone calculated at 25 °C. Polymer solutions were allowed to equilibrate for 12 h at 25 °C before measurements. The viscosity of each solution was calculated from the average of five repeated measurements.

The specific viscosity η_{sp} was calculated according to the following equation

$$\eta_{sp} = \frac{\nu - \nu_0}{\nu_0} \quad (1)$$

where ν_0 is the kinematic viscosity of acetone and ν is the kinematic viscosity of the polymer solutions employing acetone as solvent.

2.2.2. Nanoparticle preparation

Nanoparticles were prepared by a modified solvent displacement method at 25 °C, as described previously (Jung et al., 2000). Polymer (with or without salbutamol) dissolved in a semipolar organic solvent was injected into a magnetically stirred (500 rpm) aqueous phase using a special apparatus. The apparatus consists

of an electronically adjustable peristaltic pump which was used to inject the organic solution into the aqueous phase through an injection needle (Fine-Ject® 0.6 × 30 mm) at a constant flow rate of 10.0 ml/min (unless specified otherwise) in order to improve the reproducibility of the process. After injection of the organic phase, the resulting colloidal suspension was continuously stirred under a fume hood for at least 5 h to allow for complete evaporation of the organic solvent. Particles were characterized and used directly after preparation.

2.2.3. Construction of ternary phase diagram

As a map of compositions a right triangle, three-component phase diagram ("ouzo diagram") was chosen, where compositions are plotted according to the mass fraction of a solute (polymer) on the abscissa and the mass fraction of a solvent (acetone) on the ordinate (Vitale and Katz, 2003). Due to low polymer mass fractions ($\leq 10^{-1}$) a logarithmic scale was adopted for the abscissa. The concentration of a third component (aqueous phase) is found by the difference. In this diagram, one can locate the metastable region where supersaturation allows the formation of stable nanoparticle suspensions. The amounts of polymer, acetone and aqueous phase were chosen to reach the desired mass fractions in the ternary system, where f_p is the mass fraction of polymer and f_a is the mass fraction of acetone.

An example experiment was carried out as follows: To achieve the intended f_p for P(VS-VA)-g-PLGA-4-10 of 0.003 and f_a of 0.2, we kept the aqueous phase volume constant at 5 ml. The mass fraction of water (f_w) of 0.797 was found by the difference ($f_w = 1 - f_p - f_a$). The corresponding mass of water can be calculated from its density at 25 °C (0.997 g/cm^3). Then we calculated the planned mass of polymer (0.01876 g) and acetone (1.2509 g) that needed to be added to the aqueous phase to meet the desired mass fractions. The density of polymer in acetone was measured in a concentration range from 2 to 60 mg/ml as described above. The determined calibration curve (density of polymer solution (g/cm^3) = 0.00042 (ml g mg^{-1} cm^{-3}) polymer concentration (mg/ml) + 0.7891 (g/cm^3); $R^2 = 0.9998$) was used in order to get an accurate measure of the mass fraction of polymer and acetone. Assuming a density of 0.7893 g/cm^3 for acetone at 25 °C, its volume could be determined. The concentration of polymer in acetone (0.0118395 g/ml) corresponded to a density of 0.79407 g/cm^3. Therefore to achieve the required mass of polymer and acetone, the volume of the polymer solution was calculated (in this case 1.599 ml). The calculated mass of polymer was dissolved in the adjusted volume of acetone prior to injection into the aqueous phase. For the construction of the phase diagram with P(VS-VA)-g-PLGA-4-10 and acetone, the aqueous phase was composed of filtrated and double distilled water (pH 7.0, conductance 0.055 μS/cm), whereas for the construction of the phase diagram with PLGA (RG502H) and acetone, the aqueous phase consisted of filtrated and double distilled water (pH 7.0, conductance 0.055 μS/cm) with the addition of 0.1% (m/v) Pluronic® F68.

2.2.4. Physicochemical characterization of nanoparticles

2.2.4.1. Particle size measurement. The average particle size and size distribution of nanoparticles were determined by photon correlation spectroscopy (PCS) using a Zetasizer NanoZS/ZEN3600 (Malvern Instruments, Herrenberg, Germany). The analysis was performed at a temperature of 25 °C using samples appropriately diluted with filtrated and double distilled water in order to avoid multiscattering events. DTS v. 5.10-software was used to calculate particle mean diameter (Z-Ave) and the width of the fitted Gaussian distribution, which is displayed as the polydispersity index (PDI). Each size measurement was performed with at least 10 runs. All measurements were carried out in triplicate directly after nanoparticle preparation.

2.2.4.2. ζ-Potential measurement. The ζ-potential was measured by laser Doppler anemometry (LDA) using a Zetasizer NanoZS/ZEN3600 (Malvern Instruments, Herrenberg, Germany). The analysis was performed at a temperature of 25 °C using samples appropriately diluted with 1.56 mM NaCl solution in order to maintain a constant ionic strength. DTS v. 5.10-software was used to calculate the average ζ-potential values from the data of multiple runs. All measurements were carried out in triplicate directly after nanoparticle preparation.

2.2.5. Atomic force microscopy

Morphology of nanoparticles was analyzed by atomic force microscopy (AFM). Samples were prepared by placing a sample volume of 10 μl onto commercial glass slides (RMS < 3 nm). The slides were incubated with the nanoparticle suspension for 10 min before washing twice with distilled water and drying in a stream of dry nitrogen. Samples were investigated within 2 h after preparation. AFM was performed using a NanoWizard® (JPK Instruments, Berlin, Germany) in intermittent contact mode to avoid damage to the sample surface. Commercially available Si_3N_4 tips attached to I-type cantilevers with a length of 230 μm and a nominal force constant of 40 N/m (NSC16 AlBS, Micromasch, Tallinn, Estonia) were used. The scan frequency was between 0.5 and 1 Hz and antiproportional to the scan size. The results were visualized as retrace signal in height mode.

2.2.6. Determination of entrapped salbutamol by high performance liquid chromatography (HPLC)

To determine the amount of entrapped salbutamol, a 1 ml sample of nanosuspension was frozen at −80 °C, thawed, and immediately centrifuged for 10 min at 13,000 × *g* (Eppendorf Centrifuge 5415C, Eppendorf, Hamburg, Germany). At this point, the supernatant was sampled to determine the amount of unencapsulated salbutamol remaining in the nanosuspension. The pellet was freeze-dried (Beta II, Christ, Osterode, Germany), weighed, and then dissolved in 450 μl of chloroform with shaking. After complete dissolution, 900 μl of acidic water (adjusted to pH 2.5 with phosphoric acid), was added to the chloroform solution, and this mixture was shaken for at least 30 min and then centrifuged for at least 5 min at 13,000 × *g* (Eppendorf Centrifuge 5415C, Eppendorf, Hamburg, Germany) to extract the salbutamol located in the top (aqueous) layer. A sample was taken from the aqueous phase to determine the amount of encapsulated salbutamol.

Salbutamol concentrations were determined by HPLC and compared to control standards undergoing the same treatments as the samples. Chromatography was carried out using a Waters Nova-Pak C18 column (150 mm × 3.9 mm, 60 Å pore size, 4 μm particle size) (Waters, Eschborn, Germany) at 35 °C, with a mobile phase flow rate of 0.6 ml/min. The mobile phase contained a mixture of 10% methanol and 90% of the following solution: 36.6 mM sodium dihydrogenphosphate + 33.4 mM triethylamine, adjusted to pH 6.0 with phosphoric acid. All samples were assayed with a Waters 486 UV detector (Eschborn, Germany) at a wavelength of 277 nm.

2.2.7. Statistics

All measurements were carried out in triplicate and values are presented as the mean ± S.D. unless otherwise noted. Statistical calculations were carried out using the software SigmaStat 3.5 (STATCON, Witzenhausen, Germany). To identify statistically significant differences, one-way ANOVA with Bonferroni's post *t*-test analysis was performed. Probability values of $p < 0.05$ were considered significant.

3. Results and discussion

3.1. Effects of physicochemical properties on nanoparticle preparation

Due to considerable interest in biodegradable nanoparticles as drug delivery systems and progress in the field of pharmaceutical nanotechnology over the past decades, different strategies have been proposed for the production of polymeric nanoparticles, allowing extensive modulation of their characteristics (Quintanar-Guerrero et al., 1998; Galindo-Rodriguez et al., 2004; Vauthier and Bouchemal, 2009). Among the numerous manufacturing strategies, the solvent displacement method is known to be a convenient technique for the production of biodegradable nanoparticles. The addition of polymer dissolved in a semipolar organic solvent to an aqueous phase leads to precipitation of polymer in the form of colloidal particles. The mechanism of particle formation has been explained by interfacial turbulences between the two liquid phases which are governed by the Marangoni effect (Sternling and Scriven, 1959; Quintanar-Guerrero et al., 1998; Galindo-Rodriguez et al., 2004). Accordingly, the originally elliptically shaped structure of the injected solvent layer breaks down into small droplets which again break down into smaller and smaller parts until non-divisible polymer aggregates are left, thereby allowing reproducible production of polymeric nanoparticles with narrow size distributions. Important parameters determining the success of the method and affecting the physicochemical properties of the nanoparticles are the miscibility of the semipolar organic solvent with water (or whichever third component is used to cause polymer precipitation) and the nature of the polymer/solvent/water interactions. Optimal conditions for nanoprecipitation were described when the polymer was dissolved in a theta solvent that has a solubility parameter close to that of water and when the polymer concentration dissolved in the semipolar organic solvent remained in a diluted state (Galindo-Rodriguez et al., 2004; Legrand et al., 2007).

The effect of different solvents on nanoparticle production was studied by comparing the results obtained using acetone to those obtained using acetonitrile and tetrahydrofuran (THF) as solvents. Both water and PLGA are completely miscible in all three solvents. PLGA (RG502H) was dissolved at a concentration of 10 mg/ml in the different solvents and 1 ml of each solution containing the polymer was injected at a constant flow rate of 3.5 ml/min into 5 ml of water. The mean sizes of nanoparticles formed with acetone, acetonitrile and THF were measured after complete evaporation of the organic solvent and amounted to 140.0 ± 5.2, 148.3 ± 4.0 and 184.7 ± 5.5 nm (mean ± S.D., $n = 3$), respectively. The particle size obtained using acetonitrile as solvent is very similar to that obtained using acetone, whereas the particle size obtained using THF is significantly larger than that obtained using acetone ($p < 0.05$). This result suggests that critical parameters for nanoparticle formation are on the one hand the velocity of diffusion and on the other hand the viscosity of the organic solvent (Table 1). Since acetone and acetonitrile have higher diffusion coefficients and lower viscosities compared to THF, smaller nanoparticles are formed due to faster solvent diffusion (Jung et al., 2000).

Table 1
Physicochemical properties of solvents used in this study at 25 °C.

Solvent	Viscosity [mPa*s][a]	Binary liquid diffusion coefficient in water [$\times 10^{-5}$ cm^2/s][a]
Acetone	0.306	1.28
Acetonitrile	0.369	1.26 (15 °C)
Tetrahydrofuran	0.456	1.08

[a] Values were taken from Lide (1997) and Leaist et al. (2000).

Another important parameter associated with nanoparticle preparation by the solvent displacement method is the mixing process of the organic phase containing the polymer with the aqueous phase. The preferred way to prepare nanoparticles by solvent displacement consists in rapid injection of the organic phase into the aqueous phase (Fessi et al., 1989; Molpeceres et al., 1996; Jung et al., 2000). To address this issue, PLGA (RG502H) was dissolved at a concentration of 4 mg/ml in acetone and 1 ml of this solution was injected at different flow rates of 3.5, 7.1 and 10.6 ml/min, respectively, into 5 ml of water containing 0.1% (m/v) Pluronic® F68. It was observed that faster mixing of the organic phase containing the polymer with the aqueous phase led to a reduced mean size of the resulting colloidal particles. While at a flow rate of 3.5 ml/min, the nanoparticles had a mean particle size of 142.2 ± 4.0 nm (mean ± S.D., $n = 3$), nanoparticles prepared at a flow rate of 10.6 ml/min were significantly smaller (121.1 ± 0.4 nm) (mean ± S.D., $n = 3$) ($p < 0.05$).

Similar results were found for the preparation of nanoparticles made of poly(caprolactone) and poly(2-sulfobutyl-vinyl alcohol)-*graft*-poly(lactide-*co*-glycolide) by the solvent displacement method (Molpeceres et al., 1996; Jung et al., 2000). The critical parameter determining the particle size seems to be the velocity of diffusion of the organic solvent through the interface. With higher velocities of diffusion smaller nanoparticles are obtained. A higher solvent front kinetic energy causes a higher degree of polymer/acetone droplet dispersion in the aqueous phase, thereby decreasing the local polymer/acetone droplet concentration in the aqueous phase. A lower concentration of polymer/acetone droplets in the aqueous phase causes lower local acetone concentrations and a higher velocity of diffusion, thus resulting in smaller particles. In addition, the formation of smaller particles employing an increased solvent front kinetic energy is favored by reinforced dispersion of the injected solvent layer due to the increased shear force at the injection site.

Before we compared the influence of different PLGAs for nanoparticle production as a function of viscosity and polymer molecular weight, we performed kinematic viscosity measurements in acetone to ensure homologous chemical structure of the employed PLGA polymers. A second purpose of these measurements was to evaluate the interaction between solvent and polymer to verify the performance of acetone as solvent for PLGA. Plotting reduced viscosity η_{sp}/c versus polymer concentration c as a function of PLGA molecular weight yielded straight lines. These linear relationships are in agreement with the following equation

$$\frac{\eta_{sp}}{c} = [\eta] + k'[\eta]^2 c \quad (2)$$

where $[\eta]$ and k' are the intrinsic viscosity and the interaction constant, respectively (Thioune et al., 1997; Legrand et al., 2007). Extrapolation of the η_{sp}/c value to zero gave $[\eta]$, while k' values were calculated from the slopes of the resulting lines of regression. For the linear polyesters RG502H, RG503H, and RG504H, we calculated $[\eta]$ values of 0.16, 0.27 and 0.36 dl/g, respectively, and k' values of 0.5, 0.5 and 0.6, respectively. As expected, solutions of the different PLGA polymers in acetone led to almost similar interaction constants (k'), confirming that the PLGA polymers used in this study possessed a similar chemical structure and their interactions with acetone were independent of chain length, a characteristic feature of flexible polymers in "good" solvents (Legrand et al., 2007). Moreover, Schenderlein et al. (2004) reported the total solubility parameter for PLGA (molar ratio: lactide:glycolide = 50:50) to be between 19.9 and 23.1 MPa$^{1/2}$, indicating that acetone is a "good" solvent for this type of polymer.

To investigate the influence of polymer molecular weight (12 kDa for RG502H, 34 kDa for RG503H and 48 kDa for RG504H

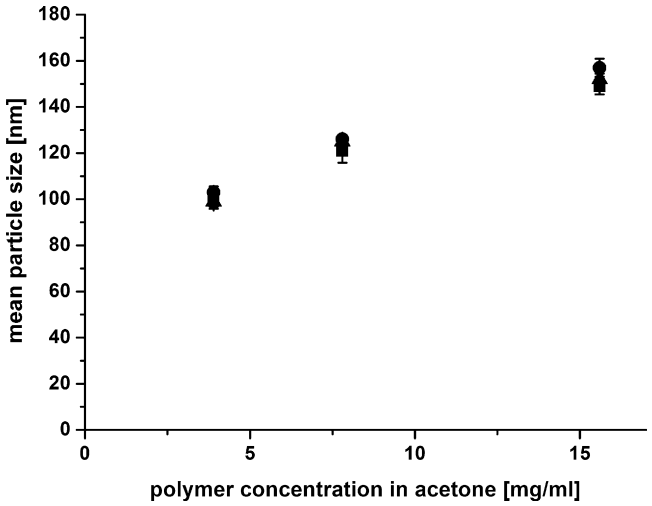

Fig. 1. Effect of poly(D,L-lactide-*co*-glycolide) (PLGA) concentration in acetone on the mean size of nanoparticles prepared by the solvent displacement method. Three PLGA polymers, RG502H (■), RG503H (●), and RG504H (▲), with increasing molecular weights of 12, 34, and 48 kDa, respectively, were used. The final concentration of polymer in water was kept constant, while the concentrations of the three polymers in acetone were varied to exclusively investigate the contribution of the viscosities of the organic polymer solutions. Values are presented as the mean ± S.D. ($n = 3$).

(Herberger et al., 2003)) and viscosity of the resulting polymer solutions in acetone on nanoparticle preparation by solvent displacement, we prepared solutions with concentrations of 3.9, 7.8 and 15.6 mg/ml for each of the three polyesters. 1.59, 0.71 and 0.34 ml of the polymer solutions were added to 5 ml of water containing 0.1% (m/v) Pluronic® F68 at a constant flow rate of 10.6 ml/min, respectively. It is well known and valid for various polymers that the use of increased polymer concentrations in the organic phase increases the mean size of the resulting particles formed by solvent displacement (Thioune et al., 1997; Galindo-Rodriguez et al., 2004; Legrand et al., 2007). For our experiments the final concentration of polymer in water was kept constant (1.1–1.2 mg/ml), while the concentrations of the three polymers in acetone were varied to exclusively investigate the contribution of the viscosities of the organic polymer solutions.

It was found that the injection of polymer solutions with increased concentrations yielded larger nanoparticles (Fig. 1). This behavior is attributed firstly to the influence of the polymer concentration on the viscosity and secondly to the number of polymer molecules per unit volume of solvent (Galindo-Rodriguez et al., 2004). The solvent displacement method relies on the rapid diffusion of the solvent into the external aqueous phase, which thereby provokes polymer aggregation in the form of colloidal particles. The mechanism of particle formation is comparable to the 'diffusion and stranding' process found in spontaneous emulsification (Moinard-Checot et al., 2006). The higher the concentration of the polymer in the organic phase, the lower the velocity of diffusion owing to the increasing viscosity of the polymer solution, and the resulting particles formed from the turbulent flow of organic solvent are larger. In addition, the velocity of solvent diffusion into the aqueous phase carries more polymer chains when a larger number of polymer molecules per unit volume of solvent are present which aggregate and thus form larger nanoparticles.

The observed particle sizes for the three PLGA polymers did not differ significantly for a given polymer concentration in acetone, even though the viscosities of the polymer solutions differed substantially, as indicated by the measured [η] values. Vitale and Katz (2003) have emphasized the importance of Ostwald ripening when describing the "ouzo effect", and Sitnikova et al. (2005) have stated that Ostwald ripening "does not depend on droplet coalescence but on the diffusive transport of dissolved matter through the dispersion medium". Equations governing the rate of diffusion-controlled Ostwald ripening include parameters such as the diffusion coefficient, aqueous molar solubility, interfacial tension, molar density, and temperature (Taylor, 1995). While the more viscous solutions containing higher molecular weight polymer in acetone would be expected to have a lower diffusion rate, the rate of Ostwald ripening for the more viscous solutions would also be lower, thereby affecting the final nanoparticle diameters.

Upon comparison of the results from these investigations regarding the viscosity of solutions of polymers of different molecular weights in the same solvent to the aforementioned investigations of the viscosity of polymer solutions in different solvents, it is likely that the contribution of the aqueous solubility of the polymer solution in the different solvents is also an important parameter. Overall, these results seem to indicate that the polymer concentration (more specifically, the mass fraction of polymer molecules divided by the mass fraction of solvent) has a more important effect upon particle size than the contribution of viscosity. Further analysis concerning the effect of PLGA (RG502H) concentration in acetone on mean sizes of nanoparticles formed by solvent displacement will be given later.

Previous publications invoking the Marangoni effect as an explanation for the formation of nanoparticles with the solvent displacement method have described the importance of interfacial tension in causing gradients leading to nanoprecipitation. Therefore, we monitored the influence of the interfacial tension on the nanoparticle preparation process in two ways. Both methods led to a decrease of the interfacial tension of the aqueous phase. The first method was accomplished by an addition of different amounts of the surfactant Pluronic® F68 to the aqueous phase. In this context we prepared aqueous solutions having amphiphilic non-ionic triblock copolymer concentrations (0–5%, m/v) below, at and above the critical micelle concentration (~1%, m/v) (Batrakova et al., 1998). The injection of 1 ml of PLGA (RG502H) in acetone (4 mg/ml) at a flow rate of 10.6 ml/min into 5 ml of aqueous phase containing different amounts of surfactant led to the formation of colloidal particles with mean diameters of approximately 130 nm independent of the concentration of surfactant added to the aqueous phase. This is in agreement with previous investigations in which surfactant concentrations above the critical micelle concentration did not significantly affect particle size (Molpeceres et al., 1996).

To assess the contribution of interfacial tension in the ternary system composed of PLGA (RG502H), acetone, and water, we employed a second method which, to our knowledge, has not been previously described in this context. This method consisted of injecting the polymer solution into either pure water or into a mixture of water and acetone. The mixture of acetone and water has a lower interfacial tension than pure water, meaning that if interfacial tension plays an important role in the particle formation process this should be evident in the characteristics of particles prepared by this method.

Table 2 shows particle properties upon injection of the polymer solution into pure water or water premixed with acetone. With a decrease in the interfacial tension caused by the addition of surfactant or premixing acetone with water prior to injection of the polymer solution, one would expect that this would lead to faster mixing, less resistance to solvent diffusion, resulting in a smaller particle size. However, no significant difference in particle size was observed, which confirms that interfacial tension does not significantly influence the conditions for nanoparticle formation by the solvent displacement method. Finally, the above mentioned results give evidence that the preparation of nanoparticles by the solvent displacement method is in agreement with principles described by

Table 2
Contribution of interfacial tension in the ternary system composed of poly(D,L-lactide-*co*-glycolide) PLGA (RG502H), acetone, and water on nanoparticle formation by solvent displacement. The polymer solution was injected into either pure water or into a mixture of water and acetone. Values are presented as the mean ± S.D. ($n = 3$).

PLGA in acetone [mg/ml]	Volume polymer solution [ml]	Volume premixed acetone [ml]	Volume water [ml]	Particle size [nm]	PDI	ζ-Potential [mV]
16	1.0	–	5.0	175.7 ± 5.7	0.101 ± 0.017	−35.0 ± 0.3
16	0.5	–	5.0	174.5 ± 7.6	0.081 ± 0.024	−43.3 ± 0.4
16	0.5	0.5	5.0	181.3 ± 7.9	0.072 ± 0.009	−36.7 ± 0.6
8	1.0	–	5.0	144.9 ± 1.7	0.100 ± 0.019	−29.4 ± 0.6
8	0.5	–	5.0	148.6 ± 1.0	0.165 ± 0.014	−44.7 ± 1.8
8	0.5	0.5	5.0	150.9 ± 1.8	0.093 ± 0.018	−40.6 ± 1.0

the "ouzo effect". The observed particle sizes and particle size distributions are almost constant and independent of the amount of surfactant and/or solvent used (Ganachaud and Katz, 2005).

3.2. Phase diagrams for blank nanoparticles composed of PLGA (RG502H) and P(VS-VA)-g-PLGA-4-10

In the past, authors proceeded by trial and error to find the operating window for the production of thermodynamically stable polymeric nanoparticles by the solvent displacement method. Hence, only limited information showing the metastable region on ternary phase diagrams – the conditions for the formation of stable nanoparticle suspensions from polymers useful for drug delivery – are available (Stainmesse et al., 1995). This metastable region corresponds to the "ouzo region" as presented by Vitale and Katz (2003). They have demonstrated this using a ternary system consisting of a hydrophobic solute (divinyl benzene), a solvent (ethanol) and a non-solvent (water) based on a nucleation and growth process. Polymers can also act as hydrophobic solute molecules and the "ouzo effect" applies to the formation of nanoparticles (Ganachaud and Katz, 2005). The formation of stable nanoparticles occurred when a polymer is rapidly brought into the metastable region between the binodal (miscibility-limit curve) and spinodal (stability-limit curve) boundaries in a ternary phase diagram. This concept was used recently to characterize the "ouzo region" for poly(methyl methacrylate) (Aubry et al., 2009). Since this type of polymer is just a model and has only limited relevance for drug delivery, we employed the linear polyester PLGA (RG502H), and the newly synthesized, negatively charged branched polyester P(VS-VA)-g-PLGA-4-10, suitable for nanoparticle production (Rytting et al., 2008).

Fig. 2a shows the experimentally determined metastable "ouzo region" for our ternary system composed of PLGA (RG502H), acetone, and water (containing 0.1% (w/v) Pluronic® F68) at 25 °C. The phase diagram was constructed by adding various polymer/solvent mixtures to the aqueous phase. At specified concentrations, the amounts of polymer, solvent, and water fall into a thermodynamically metastable region ("ouzo region") in the phase diagram, and stable polymeric nanoparticles are formed. This partial phase diagram shows that the "ouzo region" (closed squares) is very narrow with respect to the final polymer weight fractions and will not be well represented by a complete ternary phase diagram. Therefore, only the magnified left part of the triangular phase diagram is presented as a right triangle phase diagram ("ouzo diagram") using a logarithmic scale for the mass fraction of polymer. The open triangles show the experimentally determined miscibility limits of the polymer in the aqueous phase. These mixtures appear as transparent single phases. The left boundary (binodal curve) represents the log-linear cosolvent enhancement of the aqueous solubility of the polymer with increasing amounts of acetone (Yalkowsky et al., 1972). The onset of the "ouzo effect" can be derived by visual observations from the change of transparent solutions to turbid nanosuspensions, which always occurred immediately after the components were brought into contact. The "ouzo region" represents the thermodynamically metastable region between the binodal and spinodal curves in the phase diagram where stable polymeric nanoparticles are formed. The right boundary (spinodal curve) represents the precipitation of the polymer due to insolubility and transgression of the "ouzo region" where supersaturation allows the formation of stable nanoparticles. Upon pouring an excess of dissolved polymer into water, large particles arising from spinodal decomposition were formed in addition to nanoparticles (Ganachaud and Katz, 2005; Aubry et al., 2009). The onset of spinodal decomposition can be determined visually from the change of turbid nanosuspensions to the formation of polymer pellets and polymer aggregates that stick to the injection needle, magnetic stirrer, and flask.

The sizes of nanoparticles in the final suspensions prepared inside the "ouzo region" were measured systematically using PCS after complete evaporation of the organic solvent. The particle sizes ranged from 59 to 223 nm. All nanoparticle suspensions had a narrow size distribution (PDI < 0.3). Thus, the use of an "ouzo diagram" as a map of compositions of polymer, solvent and non-solvent is a beneficial tool to produce nanoparticles with specified physicochemical properties. Next, we measured the mean diameter of nanoparticles prepared inside the "ouzo region" as a function of PLGA mass fraction for three mass fractions of acetone (f_a) of 0.1, 0.2, and 0.3, respectively (Fig. 2b). At fixed PLGA concentrations, increasing the amount of acetone caused the mean particle diameter to decrease. Conversely, at fixed acetone concentrations, increasing the amount of PLGA caused the mean particle diameter to increase.

The log–log representation of each series showed that the mean particle diameter varied as a power law of PLGA mass fraction ($R^2 > 0.99$). The slopes of the resulting lines of regression were close to 1/3 (0.33, 0.31, and 0.35), indicating that the volume per particle was proportional to the amount of PLGA in the initial solution, as claimed by Aubry et al. (2009). Moreover, a log–log plot of the mass fraction ratio of PLGA and acetone versus mean particle diameter yielded one straight line, showing curves in the data from Fig. 2b collapsed to form a single line in Fig. 2c ($R^2 > 0.99$), indicating that the mean size of nanoparticles formed depends only on the excess of polymer to acetone in the system and is not a function of the mass fraction of acetone. The slope of the resulting line of regression was found to be 1/3.

Fig. 3a shows the experimentally determined metastable "ouzo region" for our ternary system composed of P(VS-VA)-g-PLGA-4-10, acetone, and water at 25 °C. The location of the "ouzo region" was comparable to that of PLGA regarding the mass fractions of polymer, solvent, and water. The sizes of the nanoparticles in the final suspensions prepared inside the "ouzo region" ranged from 60 to 163 nm with PDIs below 0.2 after complete evaporation of the organic solvent. Trends similar to PLGA were observed for the mean diameter of nanoparticles prepared inside the "ouzo region" as a function of P(VS-VA)-g-PLGA-4-10 mass fraction for different mass fractions of acetone (f_a) (Fig. 3b). A photograph of nanosuspensions

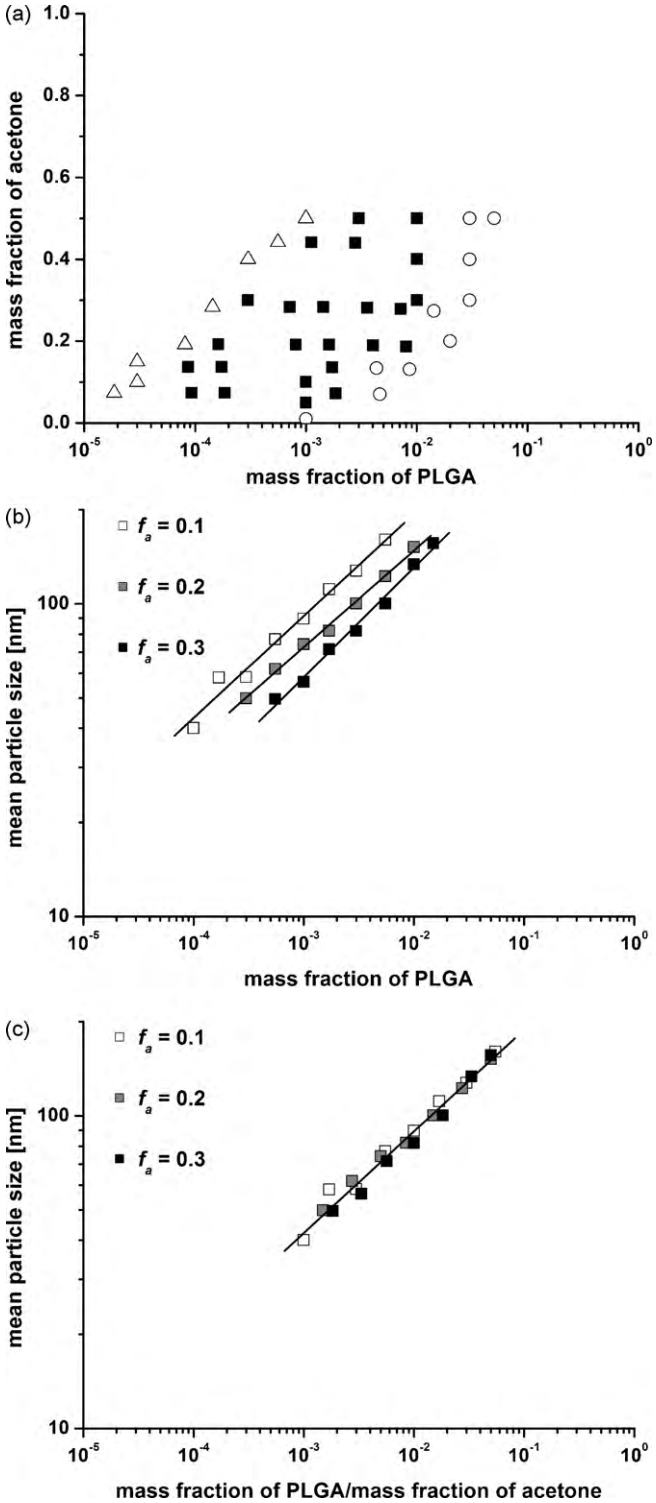

Fig. 2. Right triangle phase diagram for the ternary system poly(D,L-lactide-*co*-glycolide) PLGA (RG502H)/acetone/water (containing 0.1%, (w/v) Pluronic® F68) at 25 °C (Δ – one phase region, ■ – stable "ouzo region", and ○ – unstable "ouzo region") (a), mean particle size as a function of the mass fraction of PLGA in different mass fractions of acetone (f_a) (b), and mean particle size as a function of the mass fraction ratio of PLGA and acetone (c). The straight lines in (b) and (c) represent linear fits of the experimental data ($R^2 > 0.99$).

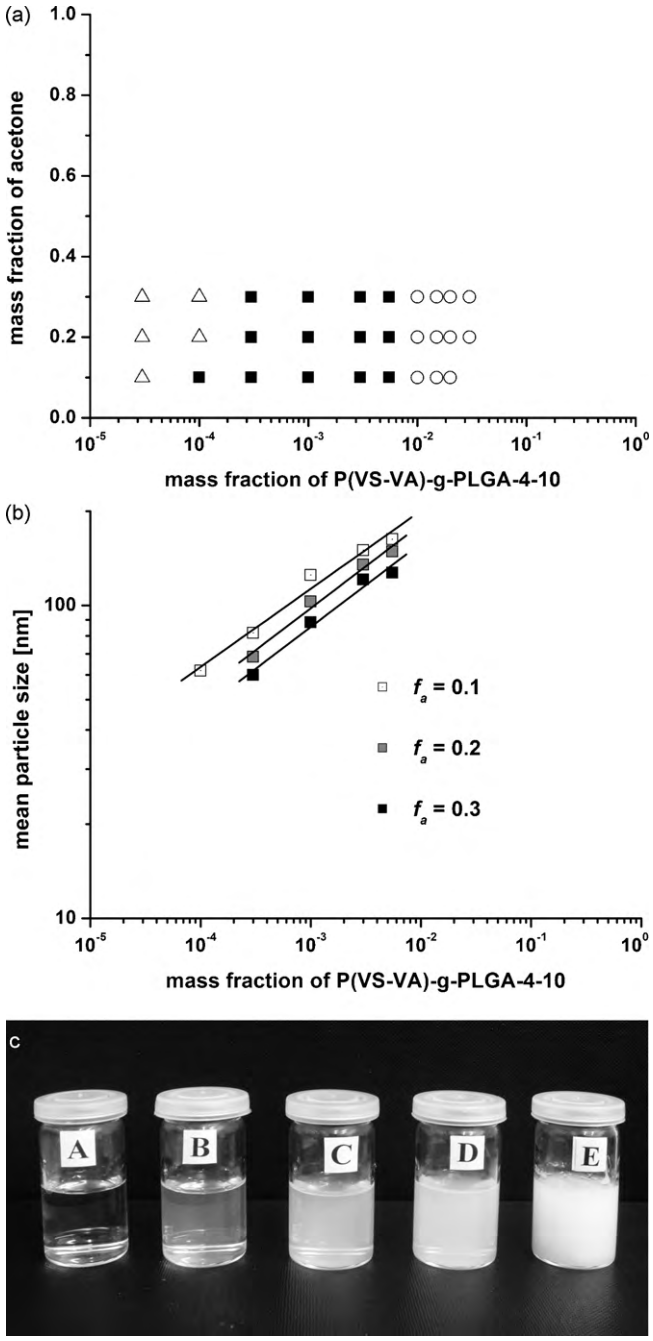

Fig. 3. Right triangle phase diagram for the ternary system poly(vinyl sulfonate-*co*-vinyl alcohol)-*graft*-poly(D,L-lactide-*co*-glycolide)-4-10/acetone/water at 25 °C (Δ – one phase region, ■ – stable "ouzo region", and ○ – unstable "ouzo region") (a), mean particle size as a function of the mass fraction of polymer in different mass fractions of acetone (f_a) (b), and a photograph of nanosuspensions with increasing polymer mass fractions ((A) 0.00003, (B) 0.001, (C) 0.003, (D) 0.0055 and (E) 0.03), while keeping the mass fraction of acetone constant at 0.2 (c). The straight lines in (b) represent linear fits of the experimental data ($R^2 > 0.98$).

with different amounts of polymer, solvent, and water is presented in Fig. 3c. The mass fraction of acetone was kept constant at 0.2, while the polymer mass fractions increased ((A) 0.00003, (B) 0.001, (C) 0.003, (D) 0.0055, and (E) 0.03). A transparent single phase indicating the miscibility of the polymer in the aqueous phase is shown in (A). Increasing the mass fraction of polymer ((B)–(D)) led to turbid nanosuspensions inside the "ouzo region". Further increase of the mass fraction of polymer enhanced the formation of visible aggregates (E).

3.3. Shift in the "ouzo region" for P(VS-VA)-g-PLGA-4-10 upon drug loading

Since for successful treatment of diseases, nanoparticles need to be loaded with drug (Soppimath et al., 2001; Panyam and Labhasetwar, 2003), we repeated the phase diagram measurements for P(VS-VA)-g-PLGA-4-10 after the addition of a positively charged model drug. Salbutamol free base was chosen and used throughout the experiments. The amount of drug that can be encapsulated is dependent on the mutual solubility of the drug and polymer in acetone. In this case, the P(VS-VA)-g-PLGA polymer was observed to act as a cosolute to increase the amount of salbutamol that is soluble in acetone. The limit of the polymer's ability to enhance drug solubility in acetone is a function of theoretical drug loading. Decreased encapsulation efficiency upon increased theoretical loading was determined to be caused by decreased mutual solubility of the drug/polymer complex during the preparation process. This leads to a "solubility-limited" decrease in theoretical loading. Optimal salbutamol loading for P(VS-VA)-g-PLGA nanoparticles was achieved with 5% (w/w) theoretical loading (Rytting et al., 2010).

The experimentally determined metastable "ouzo region" for our ternary system composed of P(VS-VA)-g-PLGA-4-10 with an addition of 5% (w/w) of salbutamol, acetone, and water at 25 °C is shown in Fig. 4a. In this case, the location of the "ouzo region" was shifted to higher mass fractions of polymer compared to the "ouzo region" of PLGA and P(VS-VA)-g-PLGA-4-10 alone. The sizes of the nanoparticles in the final suspensions prepared inside the "ouzo region" ranged between 59 and 191 nm with PDIs below 0.25 after complete evaporation of the organic solvent. Similar trends compared to PLGA and P(VS-VA)-g-PLGA-4-10 were observed for the mean diameter of nanoparticles prepared inside the "ouzo region" as a function of polymer mass fraction for different mass fractions of acetone (f_a) (Fig. 4b). Nanoparticles inside the "ouzo region" were visualized by AFM and showed spherical shape (Fig. 4c). The size data from AFM were in agreement with the data from PCS. The observed shift in the "ouzo region" results from the increased solubility of the polymer in water due to its complexation with drug. This increased solubility leads to a different pattern in the "ouzo region" and means that substantial adjustments of polymer concentrations would be necessary to produce drug-loaded nanoparticles with the same size characteristics as blank nanoparticles from the same polymer.

Fig. 5 displays the log–log plot of the mass fraction ratio of P(VS-VA)-g-PLGA-4-10 (without (a) and with drug (b)) and acetone versus mean particle diameter. The points of the curves

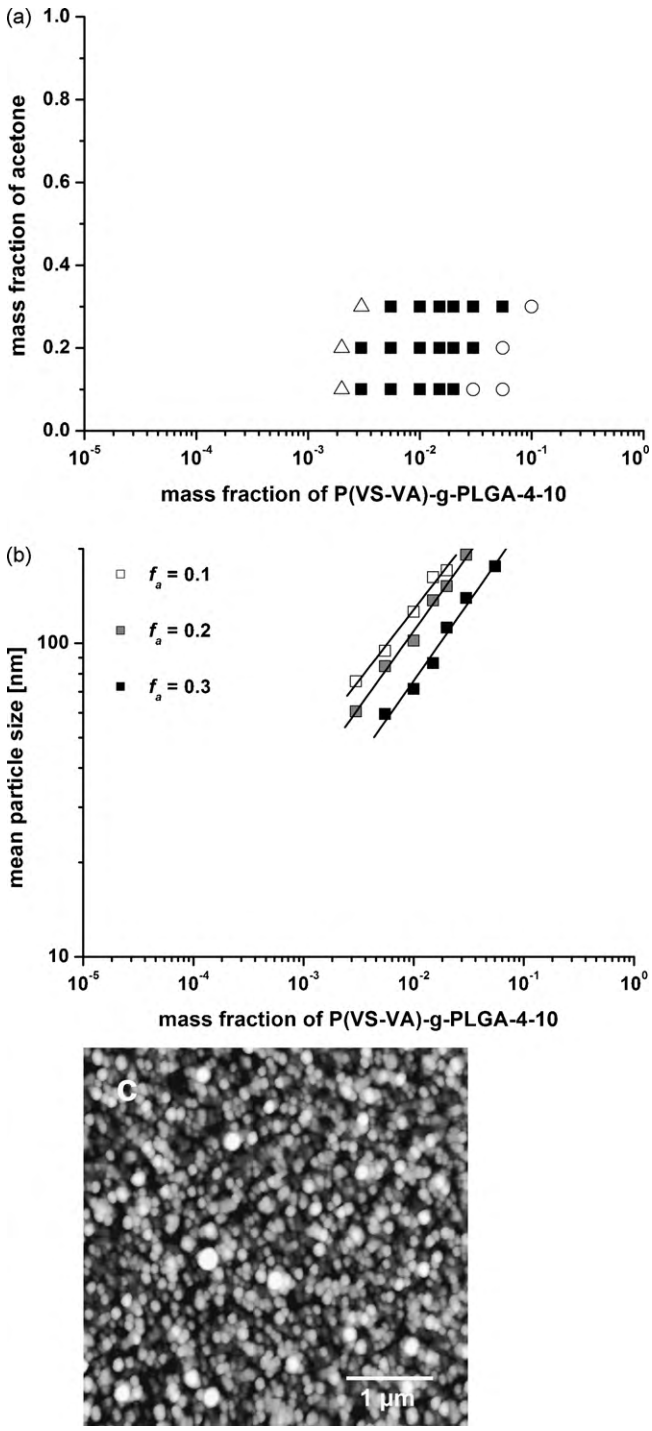

Fig. 4. Right triangle phase diagram for the ternary system poly(vinyl sulfonate-*co*-vinyl alcohol)-*graft*-poly(D,L-lactide-*co*-glycolide)-4-10 +5% (w/w) of salbutamol/acetone/water at 25 °C (Δ – one phase region, ■ – stable "ouzo region", and ○ – unstable "ouzo region") (a), mean particle size as a function of the mass fraction of polymer in different mass fractions of acetone (f_a) (b), and an atomic force microscopy image of nanoparticles prepared at a polymer mass fraction of 0.01 and an acetone mass fraction of 0.2 (c). The straight lines in (b) represent linear fits of the experimental data ($R^2 > 0.98$).

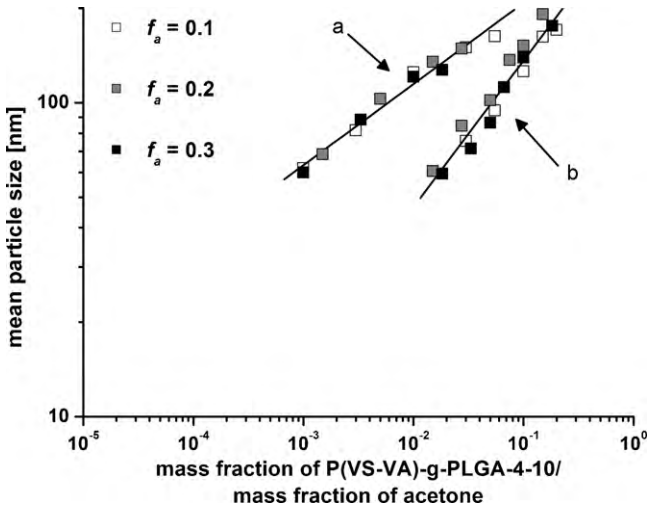

Fig. 5. Log–log plot of the mass fraction ratio of poly(vinyl sulfonate-*co*-vinyl alcohol)-*graft*-poly(D,L-lactide-*co*-glycolide)-4-10 (without (a) and with +5%, (w/w) salbutamol (b)) and acetone versus mean particle diameter. The straight lines represent linear fits of the experimental data ($R^2 > 0.97$).

in Figs. 3a and 4b again collapse to form single straight lines ($R^2 > 0.97$). The slopes of the resulting lines of regression were again found to be close to 1/3 (0.26 and 0.47), indicating that the mean size of nanoparticles formed from the newly synthesized, negatively charged branched polyester P(VS-VA)-g-PLGA-4-10 depends only on the excess of polymer to acetone in the system and is not a function of the mass fraction of acetone.

The usefulness of the solvent displacement method is often limited to lipophilic drugs that are highly soluble in polar organic solvents, but only slightly soluble in water, to avoid extensive loss of the drug into the aqueous phase during nanoparticle formation. Encapsulation of water soluble drugs is a difficult task, due to the low affinity of the drug compounds to the polymers on the one hand, and the short distances drugs have to cover to diffuse out of the particles on the other hand (Barichello et al., 1999). Thus, poor incorporation of the low molecular weight hydrophilic drug salbutamol into nanoparticles prepared from the hydrophobic polymer PLGA had been observed (Hyvoenen et al., 2005; Helle et al., 2008). The solvent selection and addition of different excipients

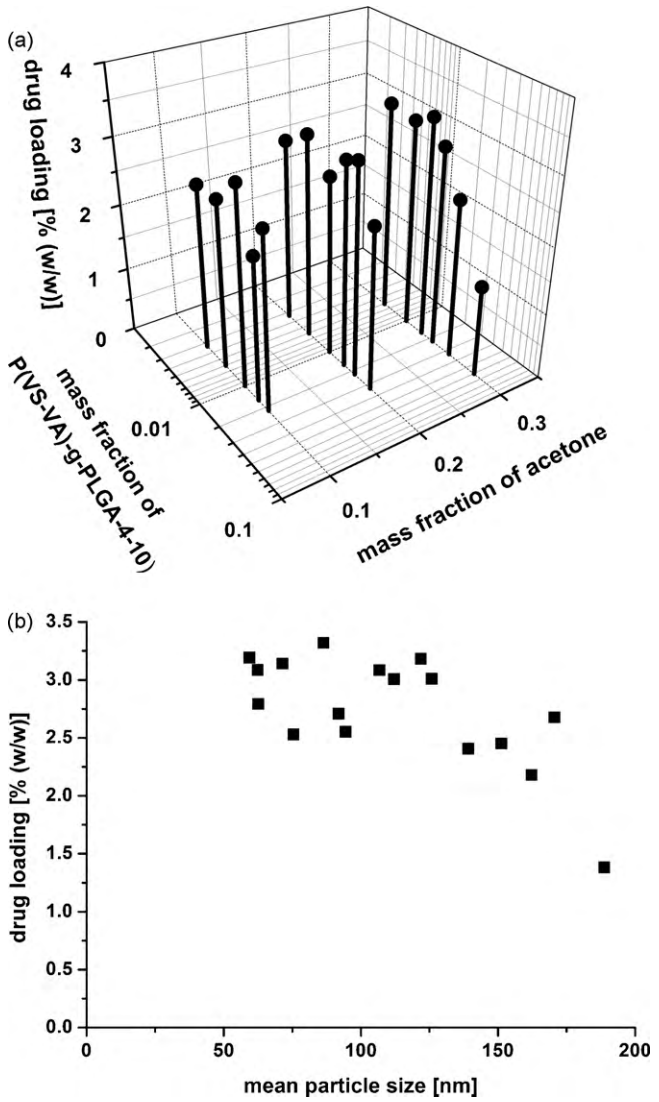

Fig. 6. Drug loading (a) and the correlation between size and drug loading (b) for nanoparticles prepared inside the "ouzo region" from the newly synthesized, negatively charged branched polyester poly(vinyl sulfonate-*co*-vinyl alcohol)-*graft*-poly(D,L-lactide-*co*-glycolide)-4-10 by solvent displacement. The theoretical salbutamol loading was 5% (w/w).

to the inner organic phase, like surfactants, were found to improve encapsulation efficiency. Similar results were possible by manipulating the outer water phase by pH changes or the addition of salts (Govender et al., 1999; Peltonen et al., 2004). However, these methods were not considered for the preparation of salbutamol-loaded nanoparticles by the solvent displacement method used in this study. Rather, our approach included the synthesis of a novel class of biodegradable branched polyesters suitable for nanoparticle production (Wang et al., 2008). The introduction of negatively charged functional groups within the polymer structure of P(VS-VA)-g-PLGA promotes electrostatic interactions with oppositely charged drugs, thereby improving the design of biodegradable polymeric nanoparticulate drug delivery systems (Beck-Broichsitter et al., 2010; Rytting et al., 2010). The observed shift in the "ouzo region" upon drug loading emphasizes this strategy.

Drug loading data for the nanoparticles inside the "ouzo region" were analyzed systematically using HPLC (Fig. 6a). Salbutamol loading ranged from 1.4% to 3.2% (w/w) for P(VS-VA)-g-PLGA-4-10 nanoparticles prepared inside the "ouzo region", indicating a successful encapsulation of the hydrophilic model drug by electrostatic complexation with the charged polymer. In addition, a general trend between nanoparticle size and nanoparticle drug loading was observed, in a way that smaller particles exhibited higher drug loadings (Fig. 6b). As described above, these novel branched polyesters are suitable for the production of polymeric nanoparticles by the solvent displacement method. Owing to their amphiphilic character, no artificial surfactant is needed during nanoprecipitation. Since the surface properties of nanoparticles will not be masked by adsorbed surfactant molecules, their absence during nanoparticle preparation will be an advantage in drug loading by adsorption. The corresponding surface charge (ζ-potential) of nanoparticles was found to be below −50 mV. Since smaller particles display higher total surface areas compared to larger particles, they are able to adsorb more of the positively charged model drug onto their surface by electrostatic interactions.

4. Conclusions

Nanoparticle preparation by the solvent displacement method is in agreement with the physicochemical principles of the "ouzo effect", but interfacial tension did not influence the process as would be expected if chiefly described by Marangoni convection. In these experiments, interfacial tension was not shown to be the significant determinant affecting particle properties. "Surface tension-driven flow" is one of the primary factors describing Marangoni convection. Although interfacial tension is also a component of the Ostwald ripening rate equation, other factors related to the "ouzo effect" – such as diffusion and solubility – appear to be more influential in affecting nanoparticle preparation by solvent displacement. In fact, the solubility of the polymer in the aqueous phase marks a boundary of the "ouzo region" defining the conditions where formation of thermodynamically stable nanoparticles is possible.

Nanoparticle size depends primarily on the excess of polymer added into the system. The observed shift in the "ouzo region" upon drug loading results from the increased solubility of the polymer in water due to its complexation with the drug. This increased solubility leads to a different pattern in the "ouzo region", whose left boundary represents the log-linear solubility enhancement of the polymer's aqueous solubility with increasing amounts of acetone. This observed shift in the "ouzo region" upon drug loading means that substantial adjustments of polymer concentrations would be necessary to produce drug-loaded nanoparticles with the same size characteristics as the blank nanoparticles from the same polymer. This observation applies to this current investigation using the

strategy to incorporate a positively charged drug substance with a polymer which contains negatively charged functional groups. Other types of polymer–drug interactions may or may not be similarly affected. The particle size correlates with drug loading; in these nanoparticles where drug loading is brought about by electrostatic interactions between polymer and drug, smaller particles result in higher drug encapsulation.

Acknowledgements

The authors would like to thank Claudia Packhaeuser, Theresa Haas, and Ulrike Nierste for their technical assistance and helpful discussions. Thomas Betz (Department of Pharmaceutical Technology and Biopharmaceutics, Philipps-Universität Marburg) is gratefully acknowledged for his support with AFM.

This study was part of the research project NanoInhale (13N8888), which was supported by the German Ministry of Education and Research (BMBF). We want to express our sincere thanks for this grant.

References

Anderson, J.M., Shive, M.S., 1997. Biodegradation and biocompatibility of PLA and PLGA microspheres. Adv. Drug Deliv. Rev. 28, 5–24.

Aubry, J., Ganachaud, F., Cohen Addad, J.P., Cabane, B., 2009. Nanoprecipitation of polymethylmethacrylate by solvent shifting: 1. Boundaries. Langmuir 25, 1970–1979.

Barichello, J.M., Morishita, M., Takayama, K., Nagai, T., 1999. Encapsulation of hydrophilic and lipophilic drugs in PLGA nanoparticles by the nanoprecipitation method. Drug Dev. Ind. Pharm. 25, 471–476.

Batrakova, E.V., Han, H.Y., Alakhov, V.Y., Miller, D.W., Kabanov, A.V., 1998. Effects of Pluronic block copolymers on drug absorption in Caco-2 cell monolayers. Pharm. Res. 15, 850–855.

Beck-Broichsitter, M., Gauss, J., Gessler, T., Seeger, W., Kissel, T., Schmehl, T., 2010. Pulmonary targeting with biodegradable salbutamol-loaded nanoparticles. J. Aerosol Med. 23, 47–57.

Dailey, L.A., Wittmar, M., Kissel, T., 2005. The role of branched polyesters and their modifications in the development of modern drug delivery vehicles. J. Control. Release 101, 137–149.

Fessi, H., Puisieux, F., Devissaguet, J.P., Ammoury, N., Benita, S., 1989. Nanocapsule formation by interfacial polymer deposition following solvent displacement. Int. J. Pharm. 55, R1–R4.

Galindo-Rodriguez, S., Allemann, E., Fessi, H., Doelker, E., 2004. Physicochemical parameters associated with nanoparticle formation in the salting-out, emulsification-diffusion, and nanoprecipitation methods. Pharm. Res. 21, 1428–1439.

Ganachaud, F., Katz, J.L., 2005. Nanoparticles and nanocapsules created using the ouzo effect: spontaneous emulsification as an alternative to ultrasonic and high-shear devices. Chem. Phys. Chem. 6, 209–216.

Govender, T., Stolnik, S., Garnett, M.C., Illum, L., Davis, S.S., 1999. PLGA nanoparticles prepared by nanoprecipitation: drug loading and release studies of a water soluble drug. J. Control. Release 57, 171–185.

Helle, A., Hirsjaervi, S., Peltonen, L., Hirvonen, J., Wiedmer, S.K., 2008. Quantitative determination of drug encapsulation in poly(lactic acid) nanoparticles by capillary electrophoresis. J. Chromatogr. A 1178, 248–255.

Herberger, J., Murphy, K., Munyakazi, L., Cordia, J., Westhaus, E., 2003. Carbon dioxide extraction of residual solvents in poly(lactide-co-glycolide) microparticles. J. Control. Release 90, 181–185.

Hyvoenen, S., Peltonen, L., Karjalainen, M., Hirvonen, J., 2005. Effect of nanoprecipitation on the physicochemical properties of low molecular weight poly(L-lactic acid) nanoparticles loaded with salbutamol sulphate and beclomethasone dipropionate. Int. J. Pharm. 295, 269–281.

Jung, T., Breitenbach, A., Kissel, T., 2000. Sulfobutylated poly(vinyl alcohol)-graft-poly(lactide-co-glycolide)s facilitate the preparation of small negatively charged biodegradable nanospheres. J. Control. Release 67, 157–169.

Leaist, D.G., MacEwan, K., Stefan, A., Zamari, M., 2000. Binary mutual diffusion coefficients of aqueous cyclic ethers at 25 °C. Tetrahydrofuran, 1,3-dioxolane, 1,4-dioxane, 1,3-dioxane, tetrahydropyran, and trioxane. J. Chem. Eng. Data 45, 815–818.

Legrand, P., Lesieur, S., Bochot, A., Gref, R., Raatjes, W., Barratt, G., Vauthier, C., 2007. Influence of polymer behaviour in organic solution on the production of polylactide nanoparticles by nanoprecipitation. Int. J. Pharm. 344, 33–43.

Lide, D.R., 1997. Handbook of Chemistry and Physics. CRC Press, New York.

Moinard-Checot, D., Chevalier, Y., Briancon, S., Fessi, H., Guinebretiere, S., 2006. Nanoparticles for drug delivery: review of the formulation and process difficulties illustrated by the emulsion-diffusion process. J. Nanosci. Nanotechnol. 6, 2664–2681.

Molpeceres, J., Guzman, M., Aberturas, M.R., Chacon, M., Berges, L., 1996. Application of central composite design to the preparation of polycaprolacton nanoparticles by solvent displacement. J. Pharm. Sci. 85, 206–213.

Panyam, J., Labhasetwar, V., 2003. Biodegradable nanoparticles for drug and gene delivery to cells and tissue. Adv. Drug Deliv. Rev. 55, 329–347.

Peltonen, L., Aitta, J., Hyvoenen, S., Karjalainen, M., Hirvonen, J., 2004. Improved entrapment efficiency of hydrophilic drug substance during nanoprecipitation of poly(l)lactide nanoparticles. AAPS Pharm. Sci. Tech. 5, article 16.

Quintanar-Guerrero, D., Allemann, E., Fessi, H., Doelker, E., 1998. Preparation techniques and mechanism of formation of biodegradable nanoparticles from preformed polymers. Drug Dev. Ind. Pharm. 24, 1113–1128.

Rytting, E., Nguyen, J., Wang, X., Kissel, T., 2008. Biodegradable polymeric nanocarriers for pulmonary drug delivery. Expert Opin. Drug Deliv. 5, 629–639.

Rytting, E., Bur, M., Cartier, R., Bouyssou, T., Wang, X., Krüger, M., Lehr, C.M., Kissel, T., 2010. In vitro and in vivo performance of biocompatible negatively-charged salbutamol-loaded nanoparticles. J. Control. Release 141, 101–107.

Schenderlein, S., Lueck, M., Mueller, B.W., 2004. Partial solubility parameters of poly(D, L-lactide-co-glycolide). Int. J. Pharm. 286, 19–26.

Sitnikova, N.L., Sprik, R., Wegdam, G., Eiser, E., 2005. Spontaneously formed trans-anethol/water/alcohol emulsions: mechanism of formation and stability. Langmuir 21, 7083–7089.

Soppimath, K.S., Aminabhavi, T.M., Kulkarni, A.R., Rudzinski, W.E., 2001. Biodegradable polymeric nanoparticles as drug delivery devices. J. Control. Release 70, 1–20.

Stainmesse, S., Orecchioni, A.M., Nakache, E., Puisieux, F., Fessi, H., 1995. Formation and stabilization of biodegradable polymeric colloidal suspension of nanoparticles. Colloid Polym. Sci. 273, 505–511.

Sternling, C.V., Scriven, L.E., 1959. Interfacial turbulence: hydrodynamic instability and the Marangoni effect. Am. Inst. Chem. Eng. J. 5, 514–523.

Taylor, P., 1995. Ostwald ripening in emulsions. Colloids Surf. A: Physicochem. Eng. Asp. 99, 175–185.

Thioune, O., Fessi, H., Devissaguet, J.P., Puisieux, F., 1997. Preparation of pseudolatex by nanoprecipitation: influence of the solvent nature on intrinsic viscosity and interaction constant. Int. J. Pharm. 146, 233–238.

Vauthier, C., Bouchemal, K., 2009. Methods for the preparation and manufacture of polymeric nanoparticles. Pharm. Res. 26, 1025–1058.

Vitale, S.A., Katz, J.L., 2003. Liquid droplet dispersions formed by homogeneous liquid–liquid nucleation: "The ouzo effect". Langmuir 19, 4105–4110.

Wang, X., Xie, X., Cai, C., Rytting, E., Steele, T., Kissel, T., 2008. Biodegradable branched polyesters poly(vinyl sulfonate-covinyl alcohol)-graft poly(D, L-lactic-coglycolic acid) as a negatively charged polyelectrolyte platform for drug delivery: synthesis and characterization. Macromolecules 41, 2791–2799.

Yalkowsky, S.H., Flynn, G.L., Amidon, G.L., 1972. Solubility of nonelectrolytes in polar solvents. J. Pharm. Sci. 61, 983–984.